Biochemical Pharmacology, Vol. 53, 783–793, 1997.

ISSN 0006-2952/97/$17.00 + 0.00
PII S0006-2952(96)00815-5

Metabolism of the Vitamin D Analog EB1089 by Cultured Human Cells: Redirection of Hydroxylation Site to Distal Carbons of the Side-Chain*

V. Narayanaswamy Shankar,† F. Jeffrey Dilworth,† Hugh L. J. Makin,‡ Neil J. Schroeder,‡ David J. H. Trafford,‡ Anne-Marie Kissmeyer,§ Martin J. Calverley,§ Ernst Binderup§ and Glenville Jones†‖

†Department of Biochemistry, Queen's University, Kingston, Ontario K7L 3N6 Canada; ‡Department of Chemical Pathology, The London Hospital Medical College, London E1 2AD U.K.; and §Leo Pharmaceutical Products, DK-2750, Ballerup, Denmark

ABSTRACT. 1(S),3(R)-dihydroxy-20(R)-(5′-ethyl-5′-hydroxy-hepta-1′(E),3′(E)-dien-1′-yl)-9,10-secopregna-5(Z),7(E),10(19)-triene (EB1089) is a novel synthetic analog of 1α,25-dihydroxyvitamin D [1,25-$(OH)_2D_3$] with potential for use in the treatment of hyperproliferative disorders. It has an altered side-chain structure compared to 1,25-$(OH)_2D_3$, featuring 26,27 dimethyl groups, insertion of an extra carbon atom (24a) at C-24, and two double bonds at C-22,23 and C-24,24a. *In vitro* metabolism of EB1089 was studied in a human keratinocyte cell model, HPK1A-*ras*, previously shown to metabolize 1,25-$(OH)_2D_3$. Four metabolites were formed, all of which possessed the same UV chromophore as EB1089, indicating the retention of the side-chain conjugated double bond system. Two metabolites were present in sufficient quantities to identify them as 26-hydroxy EB1089 (major product) and 26a-hydroxy EB1089 (minor product), based on mass spectral analysis and cochromatography with synthetic standards. Similar metabolites were generated *in vivo* and using a liver postmitochondrial fraction *in vitro* (Kissmeyer *et al.*, companion paper). Studies with the human hepatoma Hep G2 gave rise to 2 isomers of 26-hydroxy EB1089. Studies using ketoconazole, a general cytochrome P450 inhibitor, implicated cytochrome P450s in the formation of the EB1089 metabolites. COS-1 transfection cell experiments using vectors containing CYP27 and CYP24 suggest that these cytochrome P450s are probably not involved in 26- or 26a-hydroxylation of EB1089. Other experiments that examined the HPK1A-*ras* metabolism of related analogs containing only a single side-chain double bond: 1(S),3(R)-dihydroxy-20(R)-(5′-ethyl-5′-hydroxy-hepta-1′(E)-en-1′-yl)-9,10-secopregna-5(Z),7(E),10(19)-triene (MC1473; double bond at C-22,23) and 1(S),3(R)-dihydroxy-20(R)-(5′-ethyl-5′-hydroxy-hepta-3′(E)-en-1′-yl)-9,10-secopregna-5(Z),7(E),10(19)-triene (MC1611; double bond at C-24,24a) revealed that the former compound was subject to 24-hydroxylation and the latter compound was mainly 23-hydroxylated. Metabolism experiments involving EB1089, MC1473, and MC1611 in competition with [1β-^{3}H]1,25-$(OH)_2D_3$ in HPK1A-*ras* confirmed that CYP24 is probably not involved in the metabolism of EB1089 whereas, in the case of MC1473 and MC1611, it does appear to carry out side-chain hydroxylation. Our interpretation is that the conjugated double bond system in the side-chain of EB1089 is responsible for directing the target cell hydroxylation to the distal positions, C-26 and C-26a. We conclude that EB1089 is slowly metabolized *via* unique *in vitro* metabolic pathways, and that these features may explain the relative stability of EB1089 compared to other analogs *in vivo*. BIOCHEM PHARMACOL 53;6:783–793, 1997. © 1997 Elsevier Science Inc.

KEY WORDS. EB1089; vitamin D analogs; cytochrome P450; calcitriol; 1,25-dihydroxyvitamin D_3; vitamin D metabolism

It is now well established that the active form of vitamin D_3, 1α,25-$(OH)_2D_3$,¶ has potent cell-differentiating/antiproliferative activities in addition to its role in calcium homeostasis [3]. This has led researchers in the pharmaceutical industry to search for "noncalcemic" vitamin D analogs (i.e. those that possess antitumour effects without calcemic activity). Attention has been mainly focussed upon vitamin D analogs that have modifications in the side-chain. Several side-chain-modified analogs that show favourable dissociation of effects have already been developed for clinical use, some examples being calcipotriol [4] and 22-oxa-calcitriol [5]. The homologated series of analogs

* Portions of these results were presented in abstract form at the Bone & Tooth Society Meeting, Warwick, U.K. (March 1995) [1] and the American Society for Bone & Mineral Research, Baltimore, MD, U.S.A. (September 1995) [2].

‖ Corresponding author. Dr. Glenville Jones, Department of Biochemistry, Queen's University, Kingston ONT K7L 3N6 Canada. Tel. (613)-545-2498; FAX (613)-545-2987.

¶ *Abbreviations:* D_3, vitamin D_3; OH or $(OH)_2$, hydroxy or dihydroxy; 1,25-$(OH)_2D_3$, 1α,25-dihydroxyvitamin D_3; DMEM, Dulbecco's modified Eagle's medium; DPPD, N,N′-diphenylethylenediamine; EB1089, 1(S),3(R)-dihydroxy-20(R)-(5′-ethyl-5′hydroxy-hepta-1′(E),3′(E)-dien-1′-yl)-9,10-secopregna-5(Z),7(E),10(19)-triene; HIM, hexane/isopropyl alcohol/methanol; MC1473, 1(S),3(R)-dihydroxy-20(R)-(5′-ethyl-5′hydroxy-hepta-1′(E)-en-1′-yl)-9,10-secopregna-5(Z),7(E),10(19)-triene; MC1611, 1(S),3(R)-dihydroxy-20(R)-(5′-ethyl-5′hydroxy-hepta-3′(E)-en-1′-yl)-9,10-secopregna-5(Z),7(E),10(19)-triene.

containing additional carbon atoms at the C-24 and/or C-26/C-27 positions have also been shown to possess potentially useful biological profiles [6]. In a recent study, we proposed that the increased biological activity of a certain vitamin D analog (20-epi-1α,25-$(OH)_2D_3$; MC1288) may be partially due to altered protein binding for the plasma globulin, DBP, and the target cell vitamin D receptor (VDR) as well as reduced catabolism by target cell enzymes [7]. It is well known that catabolism of 1,25-$(OH)_2D_3$ in target tissues occurs through hydroxylation at C-23 (1,23,25-$(OH)_3D_3$), C-24 (1,24,25-$(OH)_3D_3$) [8] or C-26 (1,25,26-$(OH)_3D_3$). The 23-hydroxylase and 24-hydroxylase activities associated with these reactions have recently been shown to colocalize with the same cytochrome P450, CYP24 [9].

EB1089 (Fig. 1), is a synthetic analog [10], with strong antiproliferative and differentiation-inducing effects on cancer cells [11, 12]. EB1089 has a unique side-chain structure featuring 26,27 dimethyl groups, insertion of an extra carbon atom (24a) at C-24, and two double bonds at C-22,23 and C-24,24a. The effect of such a *side-chain* conjugated double bond system on the metabolism of an analog by 23- and 24-hydroxylases has not previously been examined. In the present study, metabolism of EB1089 was investigated in HPK1A-*ras*, a human keratinocyte cell line previously shown to contain high catabolic enzyme activity [13]. In this study we set out to:

1. Examine qualitatively and quantitatively the metabolism of EB1089 in vitamin D target cells and liver cells;
2. Examine the metabolism of other analogs containing only one or the other of the side-chain double bonds of EB1089;
3. Examine whether or not the vitamin D metabolizing enzymes CYP27 and CYP24 might be involved in the metabolism of EB1089 and related analogs.

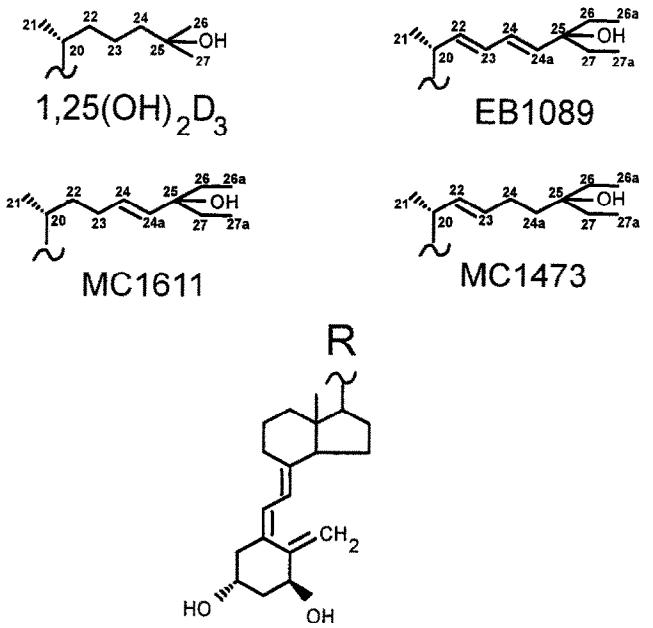

FIG. 1. Structures of EB1089 and other unsaturated, homologated vitamin D analogs. Structures of the side-chains of vitamin D analogs as compared to 1α,25-$(OH)_2D_3$, together with the ring structure of vitamin D nucleus.

MATERIALS AND METHODS

Materials

1,25-$(OH)_2D_3$ was a generous gift from Dr. M. Uskokovic (Hoffmann LaRoche, Nutley NJ). The test vitamin D analogs: EB1089, [19-^{14}C]EB1089 (56 mCi/mmol), MC1473, MC1611, as well as the chemically synthesized metabolites: EB1435, EB1445, EB1436, EB1470, and EB1446 were provided by Leo Pharmaceutical Products, Ballerup, Denmark. [1β-^{3}H]1,25-$(OH)_2D_3$ (3 Ci/mmol) was prepared earlier in our laboratory [14]. The human keratinocyte cell line [15] transfected with the *ras* protooncogene [16], HPK1A-*ras*, was the generous gift of Dr. R. Kremer (Royal Victoria Hospital, McGill University, Montreal, Québec, Canada). The hepatoma HepG2 and the SV-40 transformed African Green Monkey kidney cell line, COS-1, were obtained from the American Tissue Culture Collection (Rockville, MD). All solvents used were of HPLC grade and were supplied by Caledon (Georgetown, Ontario, Canada).

Trypsin, penicillin G, gentamycin, fungizone, and DMEM were purchased from GIBCO (Grand Island, NY). FCS was from ICN Biomedicals Inc. (Aurora, OH). DPPD was purchased from Sigma Chemical Co. (St Louis, MO) and BSA was obtained from Boehringer Mannheim, West Germany.

Cell Culture and Incubation with Vitamin D Analogs

HPK1A-*ras* were grown in DMEM supplemented with penicillin G (100 μg/mL), gentamycin (5 μg/mL), and fungizone (300 ng/mL) containing 10% FCS. Cells were maintained in 150-mm plates at 37°C in a humidified atmosphere of 5% CO_2 in air until confluence. Cells were then trypsinized and subcultured into 3 150-mm plates containing 30 mL of the medium per plate. Near confluence, 1,25-$(OH)_2D_3$ (10 nM) was added to the culture medium to induce the catabolic enzymes. After 24 hr, the medium was removed, monolayers were washed with 10 mL of PBS, and then replaced by DMEM (10 mL/plate) supplemented with 100 μM DPPD and 1% BSA. The cells were then incubated for periods of time ranging between 6 hr and 72 hr in the presence of EB1089 or MC1473 or MC1611 (to achieve a final concentration of 10 μM added in 0.01% EtOH) or [19-^{14}C]EB1089 (100 nM). The no-cell control consisted of 10 mL of the medium and the analog (10 μM in 0.01% EtOH) incubated in the absence of cells for the same length of time.

In the case of incubations with ketoconazole, HPK1A-*ras* cells were grown, induced, and processed as described above. Varying concentrations (100 nM, 1 μM, 10 μM) of ketoconazole were then added along with the substrate

EB1089 (10 μM) and incubated for 48 hr. Control experiments included all components except ketoconazole. The experiment was performed in duplicate.

Hep G2 cells were grown in Earle's minimal essential medium containing 5% FCS and antibiotics (100 μg/mL penicillin G, 5 μg/mL gentamycin, and 300 ng/mL fungizone). Cells were maintained in 150-mm plates at 37°C in a humidified atmosphere of 5% CO_2 in air until confluence. Cells were then trypsinized and subcultured into 3 150-mm plates containing 30 mL of the medium per plate. Near confluence, the medium was removed and the plates were washed with 10 mL of PBS (per plate) and then replaced by Earle's minimal essential medium (10 mL/plate) supplemented with 100 μM DPPD and 1% BSA. The cells were then incubated for 72 hr in the presence of EB1089 (10 μM in 0.01% EtOH). The no-cell control consisted of 10 mL of medium and EB1089 (10 μM in 0.01% EtOH) incubated for the same length of time.

Lipid Extraction

Cells and medium were extracted using a modification of the method of Bligh and Dyer [17], in which chloroform was replaced by methylene chloride. The methylene chloride layer was evaporated to dryness under a stream of nitrogen, redissolved in hexane/isopropyl alcohol/methanol (91:7:2, v/v/v, HIM), and subjected to purification by HPLC.

Purification of Metabolites

Analytical HPLC of metabolites of EB1089, MC1473, and MC1611 was performed on a modular system consisting of a model 590 pump, a U6K manual injector, a model 440 fixed-wavelength detector (254 nm), and a model 990 photodiode array detector (Waters Scientific, Milford, MA). EB1089 possesses the typical λ_{max} = 265 nm (ϵ ~ 17,500) expected for all vitamin D analogs possessing the *cis*-triene system, but due to the presence of conjugated double bonds in the side-chain, it has an additional λ_{max} at 235 nm (ϵ ~ 44,000). Hence, HPLC chromatograms were monitored at 235 nm and at 265 nm simultaneously, to check for the reduction of the double bonds that might lead to the formation of metabolites with only the typical vitamin D chromophore (λ_{max} = 265 nm; λ_{min} = 228 nm). Separation of metabolites was initially achieved using a 3 μm Zorbax-SIL (0.62 × 8 cm) column eluted with HIM 91:7:2 at a flow rate of 1 mL/min. Peaks showing a similar chromophore to the substrate EB1089 (λ_{max} = 265 nm; λ_{max} = 235 nm) were collected manually in glass Reactivials (Pierce, Rockford, IL) and evaporated to dryness and redissolved in HIM (88:10:2). Peaks were further purified on the same HPLC system using a Zorbax-CN (0.46 × 25 cm) column with HIM 88:10:2 at a flow rate of 1 mL/min. Again, metabolites were collected manually into glass Reactivials. This step was repeated once more to obtain metabolites sufficiently pure for mass spectral and chemical analysis.

Derivatization and Gas Chromatography-Mass Spectrometry

The technique for periodate cleavage of vitamin D analogs containing a vicinal diol and subsequent HPLC analysis of products has been described before [8]. Per-trimethylsilyl ethers of the metabolites were prepared using the reagent N-trimethylsilylimidazole and the derivatives subjected to GC-MS as previously described [18]. Mass spectra were obtained by averaging each peak and subtracting the background.

Cytochrome P450 Transfection Studies

Transfection experiments followed the standard DEAE-dextran protocol described previously [19]. Briefly, COS-1 cells were transfected with 20 μg of DNA (prepurified using Wizard maxiprep, Promega, Madison, WI) representing pSG5-based expression vectors containing either human CYP27 [20] or rat CYP24 [21]. Cells were cotransfected with 5 μg DNA representing pRSVLuc to correct for transfection efficiency. Cells were allowed to recover from vector treatment for 24 hr and then incubated with vitamin D analogs for a further 48 hr.

Rate of Catabolism of [1β-^{3}H]1,25-$(OH)_2D_3$ in the Presence and Absence of Vitamin D Analogs

The abilities of EB1089, MC1473, MC1611, and 1,25-$(OH)_2D_3$ to compete with [1β-^{3}H]1,25-$(OH)_2D_3$ for the catabolic enzymes of the side-chain oxidation pathway were assessed using a previously described procedure [22]. HPK1A-*ras* cells, suspended in DMEM without fetal calf serum but containing 0.1% BSA, were incubated with [1β-^{3}H]1,25-$(OH)_2D_3$ (23 nM) in the presence or absence of varying concentrations of analog (0 to 23 nM) for 3 hr at 37°C. Triplicate 500-μL aliquots of aqueous fraction from the cell/medium extract were mixed with aqueous scintillation fluid and the radioactivity was measured using a scintillation counter.

RESULTS

Characterization of Metabolites of EB1089 in HPK1A-ras Cells

Incubation of EB1089 with HPK1A-*ras* for 72 hr resulted in the formation of 4 metabolites (Fig. 2), all of which possessed the same UV chromophore as EB1089, suggesting retention of the side-chain unsaturation of the starting compound. These metabolites were not formed when EB1089 was incubated with medium in the absence of cells, or when cells were incubated with medium alone (data not shown). Two of the 4 metabolites, Peaks A and B, were collected in sufficient quantities to permit identification by GC-MS. Because 2 other products, labelled Peaks C and D, were formed only in trace amounts, insufficient amounts were available for identification by GC-MS.

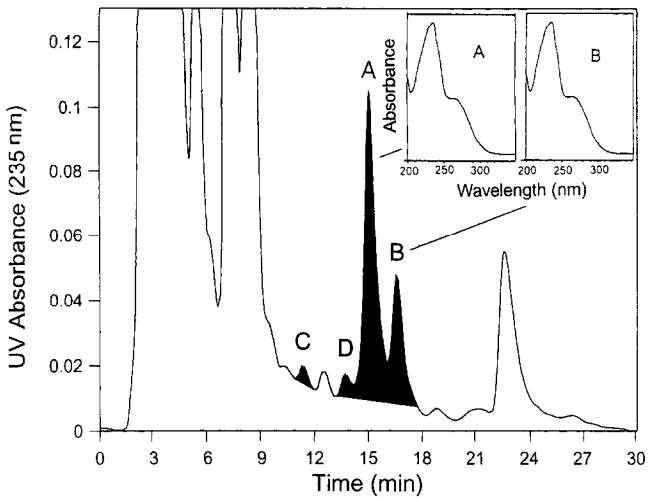

FIG. 2. HPLC profile of the lipid extract from HPK1A-ras cells incubated with EB1089. Total lipid extract was separated on a Zorbax-SIL column using the solvent HIM 91:7:2 at a flow rate of 1 mL/min. Metabolites of EB1089 were identified based upon the similarity of their chromophore (see insets) to the substrate EB1089 (λ_{max} = 235 nm) and have been shaded.

PEAK A. The mass spectrum of the pertrimethylsilylated derivative of peak A (Fig. 3a) featured a molecular ion of m/z 758, indicating a hydroxylated version of EB1089. The significant fragment m/z at 641 is due to the loss of 117 mass units, which indicates that the additional hydroxyl must be at either C-26 or C-26a. The fragility of the C25-C26 bond suggests that the hydroxyl group is probably at C26. Absence of a fragment m/z 103 also indicates that the extra hydroxyl group is not at C-26a, thereby leading to a logical conclusion that the additional hydroxyl group must be at the C-26 position. Other major fragments present in the mass spectrum include: m/z 668 $(M-90)^+$, 551 $(M-117-90)^+$, 461 $(M-117-90-90)^+$, and 371 $(M-117-90-90-90)^+$, which are the result of sequential losses of TMSiOH from the molecular ion or its major m/z 641 fragment. Fragments at m/z 743 and 729 are due to the loss of a methyl and ethyl group, respectively. A fragment at m/z 183 probably represents a cleavage across the C23-C24 bond followed by the loss of a TMSiOH group. The expected fragments at m/z 217 and 627 arise due to cleavage in the A ring. This fragmentation is found in the TMS-derivatized spectra of most 1α-hydroxylated vitamin D compounds [23].

Peak A was sensitive to periodate oxidation (Table 1), indicating the presence of vicinal hydroxyl groups (at the C-25 and C-26 positions), the cleavage product having the retention time and modified UV properties expected of an α,β,γ,δ-unsaturated ketone (λ_{max} = 270 nm). These results strongly suggest that the identity of Peak A is 26-hydroxy EB1089.

PEAK B. The mass spectrum of the pertrimethylsilylated version of Peak B (Fig. 3c) revealed a molecular ion of m/z 758, thereby indicating that this metabolite is also a hydroxylated version of EB1089. However, Peak B showed a different fragmentation pattern when compared with Peak A. A fragment at m/z 103 indicated C26-C26a fragility, thereby suggesting that the hydroxyl group is at the C-26a position. Other fragments present in the mass spectrum include: m/z 729 $(M-29)^+$, due to the loss of an ethyl group (C-27, C-27a); 668 $(M-90)^+$, due to the loss of one TMSiOH group; 639 $(M-29-90)^+$, due to the loss of one TMSiOH group from the m/z 729 fragment; 627 $(M-131)^+$ represented the cleavage in the A ring; 641 $(M-117)^+$ represented the cleavage of the C25-26 bond; 551 $(M-117-90)^+$, 461 $(M-117-90-90)^+$, and 371 $(M-117-90-90-90)^+$ are due to the result of sequential losses of TMSiOH groups. Based on these findings, Peak B was identified as 26a-hydroxy EB1089.

Comparison of Biologically Generated Metabolites of EB1089 with Chemically Synthesized Standards

The identities of metabolites Peaks A and B were confirmed by cochromatography with the authentic standards (Table 2) on both straight-phase and reversed-phase HPLC, as well as GC. 26-Hydroxy EB1089 can exist in 4 diastereomeric forms: [(25R),26R-OH-EB1089 (EB1445); (25S),26R-OH-EB1089 (EB1446); (25R),26S-OH-EB1089 (EB1470); and (25S),26S-OH-EB1089 (EB1436)]. 26a-hydroxy EB1089 can exist in 2 epimeric forms (EB1435 was synthesized as a mixture of both). Peak A, identified previously by MS as 26-hydroxy EB1089, comigrated with (25R),26R-hydroxy EB1089 (EB1445), whereas Peak B, previously identified as 26a-hydroxy EB1089, comigrated with one of the epimers within the mixture of (25R)26a-hydroxy EB1089 and (25S)26a-hydroxy EB1089 (EB1435a).

The identities of Peaks A and B were further substantiated by comparision of the mass spectra of their pertrimethylsilyl derivatives with those of the chemically synthesized standards (Fig. 3b and d). Mass spectra were found to be identical. In conclusion, Peak A is (25R)26R-hydroxy EB1089 (EB1445) and Peak B is one of the epimers of 26a-hydroxy EB1089 (EB1435a).

Rate of Metabolism of EB1089 by HPK1A-ras Cells

Figure 4 illustrates the rate of metabolism of EB1089 as compared to 1α,25-$(OH)_2D_3$ over the time period 6–72 hr. We observed a much slower disappearance of EB1089 compared to 1α,25-$(OH)_2D_3$, the difference being most pronounced at 48 hr where 60% of EB1089 remained compared with only 10% in the case of 1α,25-$(OH)_2D_3$.

Metabolism of EB1089 in Hep G2 Cells

Metabolism of EB1089 in HepG2 cells resulted in the formation of 2 metabolites (Fig. 5) both of which possessed the same UV chromophore as the substrate EB1089. The metabolites were formed only in trace amounts and, hence,

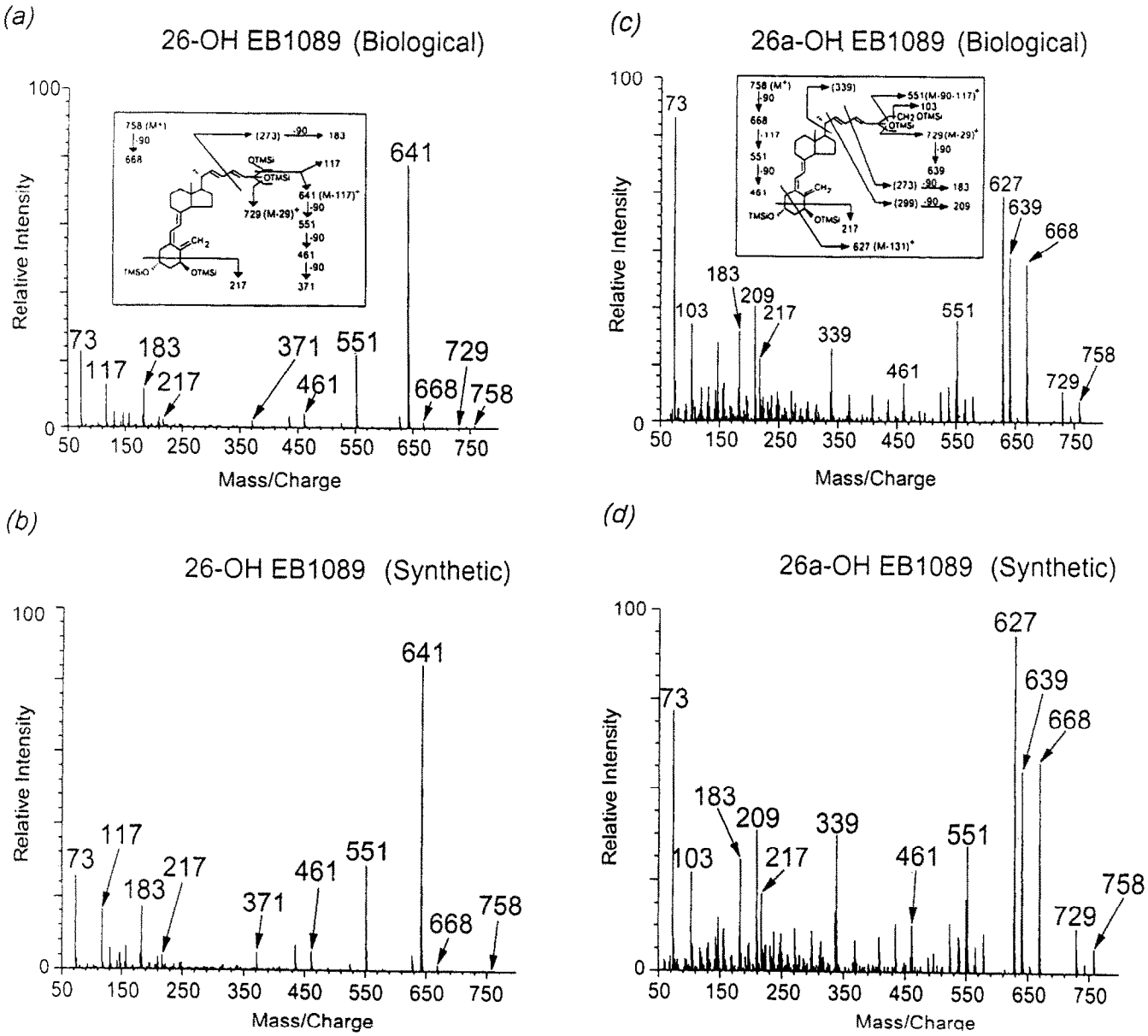

FIG. 3. Mass spectra of putative monohydroxylated metabolites of EB1089. TMSi derivatives of the purified metabolites: Peak A (a) and Peak B (c) and the corresponding synthetic standards: EB1445 (b) and EB1435 (d) were separated on an HP-1 crosslinked methyl silicone gum column with helium as a carrier gas at a flow rate of 1 mL/min. Mass spectra shown are those of the pyro-isomer and were obtained by averaging each peak and subtracting the background. The fragmentation patterns depicted are those of the actual TMSi derivatives prior to cyclization.

could not be purified in sufficient quantities to permit identification by GC-MS. HPLC performed on Zorbax-CN was able to resolve Peak A into 2 components. We found comigration of these 2 components of Peak A from HepG2 cells (Fig. 6a) with, in turn, the metabolite isolated from the HPK1A-*ras* keratinocyte cell model [(25R),26R-hydroxy EB1089; EB1445] and, second, the principal metabolite isolated *in vitro* using a rat liver postmitochondrial supernatant [(25S),26R-hydroxy EB1089; EB1446] [24] (Fig. 6b). Thus, it appears that the hepatoma cell line is capable of forming 2 of the isomers of 26-hydroxy EB1089, both of which have been isolated from other *in vitro* models.

Metabolism of [19-^{14}C]EB1089 in HPK1A-ras and HepG2 Cells

To confirm that the same metabolic pathways can operate at lower concentrations of EB1089, we performed incubations involving HPK1A-*ras* and HepG2 cells with nanomolar concentrations of [19-^{14}C]EB1089, and found that the metabolic profiles were similar to those at micromolar concentrations of substrate. Figure 7 depicts the pattern observed when [19-^{14}C]EB1089 was incubated with HPK1A-*ras* cells. A broad radioactive peak representing metabolites A and B, and comigrating with synthetic stan-

TABLE 1. Chromatographic and spectral analysis of metabolites generated from EB1089 in HPK1A-*ras* cells

	Retention time (min)		Chemical modification $NaIO_4$ cleavage*		Mass spectral analysis†		
Metabolite	Z-SIL‡	Z-CN*	Untreated	Treated	Mol. ion	Other ions	Putative identity
Peak A	15.03	13.01	12.89	9.90	758	729,668,641,551,461,371,217,183,117	26-OH EB1089
Peak B	16.55	13.67	ND§	ND§	758	729,668,639,627,551,461,217,183,103	26a-OH EB1089

* HPLC conditions: Zorbax-CN (0.46 × 0.25 cm) column eluted with HIM 88/10/2 at a flow rate of 1 mL/min; †Mass spectra of the metabolites as TMSi derivatives; ‡HPLC conditions: 3 -μm Zorbax-SIL (0.62 × 8 cm) column eluted with HIM 91/7/2 at a flow rate of 1 mL/min; §ND = not determined.

dards of 26-OH-EB1089 and 26a-OH-EB1089, was obtained.

Cytochrome P450 Inhibition Studies

To determine whether or not the enzymes involved in the metabolism of EB1089 are cytochromes, incubations of EB1089 were carried out in the presence of varying concentrations of ketoconazole (100 nM, 1 μM, 10 μM). Products were monitored and quantitated by HPLC (Fig. 8). There was significant inhibition (~45%) at 100 nM, which increased with a rise in inhibitor concentration. This inhibition was observed for Peaks A and B formed from HPK1A-*ras* cells, indicating that both the hydroxylations at carbons-26 and 26a are carried out by cytochromes P450. A closer look (Fig. 8, inset) at the ratio of the metabolites formed revealed that both the hydroxylation reactions appeared to be inhibited to the same extent.

Transfection Studies

To determine the potential involvement of the vitamin D-related cytochrome P450s, CYP24 and CYP27, in the metabolism of EB1089, transfection studies were carried out in COS-1 cells. Control experiments using 1α-OH-D_3 or 1α,25-$(OH)_2D_3$ as substrate indicated that there was considerable side-chain hydroxylation activity when cells were transfected with CYP27 or CYP24. When the transfected cells were incubated with EB1089, the levels of the 2 metabolites formed in the presence of the transfected cytochromes was not significantly different from amounts obtained when the cytochromes were absent (i.e. from endogenous hydroxylase activities present in the control transfected COS-1 cells; Fig. 9). These experiments suggest that the cytochromes P450, CYP27 and CYP24, are probably not responsible for the formation of 26- and 26a-hydroxylated EB1089 metabolites observed in keratinocyte and hepatoma cultures.

Competition of EB1089 and Related Analogs MC1473 and MC1611 for the C-24 Oxidation Pathway

The comparison of the rate of catabolism of [1β-^{3}H]1,25-$(OH)_2D_3$ in HPK1A-*ras* cells in the absence or presence of nonradioactive 1,25-$(OH)_2D_3$ or EB1089 is depicted in Fig. 10a. [1β-^{3}H]1,25-$(OH)_2D_3$ was rapidly converted to [^{3}H]-labelled water-soluble metabolites, including [1β-^{3}H] calcitroic acid. Nonradioactive 1,25-$(OH)_2D_3$ competes effectively for the enzymes involved in this pathway, leading to a reduction in the amount of [^{3}H]-labelled water-soluble metabolites. On the other hand, EB1089, over the range of concentrations tested (10^{-9} to 10^{-6} M), is inactive as an inhibitor of [1β-^{3}H] calcitroic acid production.

The ability of the analogs MC1473, MC1611 (for structures see Fig. 1), and nonradioactive 1,25-$(OH)_2D_3$ to compete with the metabolism of [1β-^{3}H]1,25-$(OH)_2D_3$ in

TABLE 2. Cochromatography of the metabolites generated from EB1089 in HPK1A-*ras* cells with synthetic standards

Compound	Relative retention time*	Relative retention time†	Relative retention time‡
(25S),26S-OH-EB1089 (EB1436)	2.64 ± 0.01	0.657 ± 0.007	1.174
(25S),26R-OH-EB1089 (EB1446)	2.59 ± 0.01	0.731 ± 0.004	1.198
(25R),26S-OH-EB1089 (EB1470)	2.60 ± 0.02	0.667 ± 0.039	1.198
(25R),26R-OH-EB1089 (EB1445)	2.73 ± 0.01	0.566 ± 0.007	1.173
Peak A	2.73 ± 0.01	0.565 ± 0.007	1.173
26a-OH-EB1089 (EB1435)	2.86 ± 0.01§	0.669 ± 0.043‖ 0.569 ± 0.001‖	1.242§
Peak B	2.88 ± 0.01	0.568 ± 0.007	1.239

* Straight-Phase HPLC conditions: Zorbax-CN (0.46 × 25 cm) column eluted with HIM 88/10/2 at a flow rate of 1 mL/min; 1α-OH-D_3 was used as the internal standard.

† Reversed-Phase HPLC conditions: Zorbax-ODS (0.62 × 8 cm) column with Eluent A: 5% MeOH in H_2O, Eluent B: 5% H_2O in MeOH; EB1089 was used as the internal standard. Gradient Program: min, 0; min, A, 30; B, 70; Flow, 1.3 mL/min; min, 30; A, 1; B, 99; Flow, 1.3 mL/min; min, 32; A, 30; B, 70; Flow, 1.3 mL/min.

‡ Gas chromatographic conditions: HP-1 crosslinked methyl silicone gum column with helium as the carrier gas at a flow rate of 1 mL/min; EB1089 was used as external standard; mean retention time = 11.425 min, n = 4.

§ Contains two unresolved isomers;

‖ Isomers resolved.

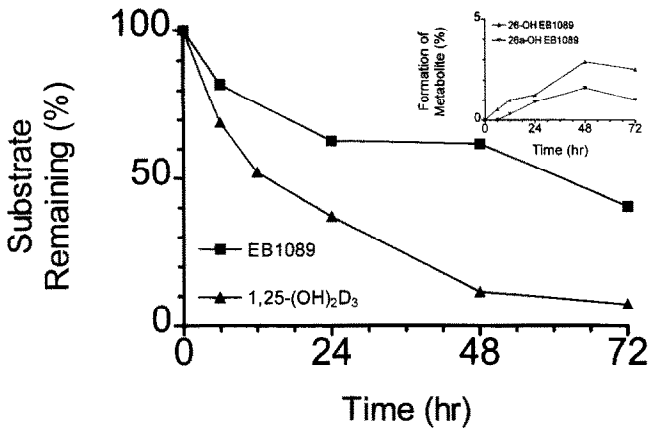

FIG. 4. Time-course of the metabolism of EB1089 incubated with HPK1A-*ras* cells. Cells were incubated with EB1089 or 1α,25-$(OH)_2D_3$ for time periods from 6 to 72 hr. The lipid extracts were subjected to HPLC to assess amounts of substrate remaining or products formed. The rate of appearance of the principal products of EB1089 is shown in the inset.

HPK1A-*ras* cells was also assessed (Fig. 10b, c). Analogs MC1473 and MC1611 have isolated double bonds at the C22–23 and C24–24a positions, respectively. It was found that both MC1473 and MC1611 competed well with 1,25-$(OH)_2D_3$, the latter compound somewhat better than the former. These results suggest that C-24 oxidation enzymes, including CYP24, could be involved in the metabolism of MC1473 and MC1611.

Characterization of the Metabolites of MC1473 and MC1611 Generated in HPK1A-ras Cells

Given that the analogs MC1473 and MC1611 were shown to compete with the C24-oxidation pathway enzymes, we thought it necessary to characterize the metabolic products that were formed from HPK1A-*ras* cells. The metabolic pattern for HPK1A-*ras* cells with MC 1473 (Fig. 11a) showed the formation of 1 major metabolite (peak A) and 2 minor metabolites (peak B split into 2 metabolites during further purification, data not shown). The mass spectrum of the pertrimethylsilylated derivative of peak A (Fig. 11b) featured a molecular ion of m/z 760, indicating a hydroxylated version of MC1473 with prominent ions at m/z 159 (cleavage between C-24a and C-25), 211 (cleavage between C-20 and C-22 followed by the loss of a silanol) and 629 $(M-131)^+$. Also observed in the mass spectrum were a

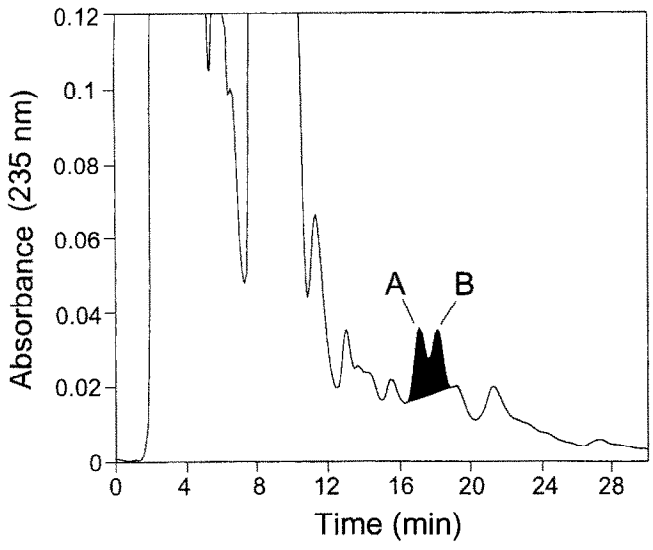

FIG. 5. HPLC profile of the lipid extract from Hep G2 cells incubated with EB1089. Total lipid extract was separated on a Zorbax-SIL column using the solvent HIM 91:7:2 at a flow rate of 1 mL/min. Metabolites of EB1089 were identified based upon similarity of their chromophore to that of the substrate EB1089 (λ_{max} = 235 nm) and have been shaded.

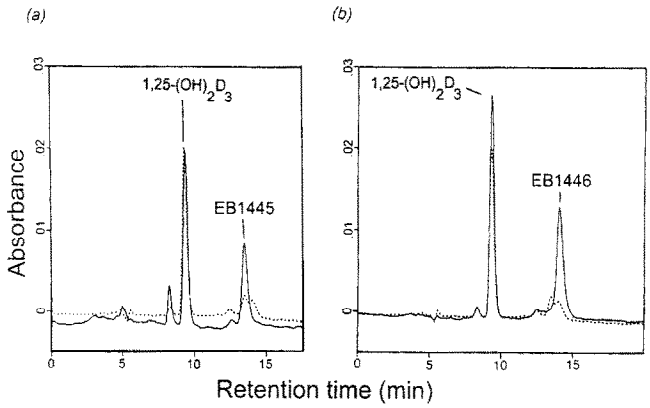

FIG. 6. Cochromatography of the two components of metabolite of EB1089 (Fig. 5, peak A) obtained from incubations in Hep G2 cells (----) with, (a) the metabolite of EB1089 obtained in HPK1A-*ras* cells (——, EB1445); (b) the metabolite of EB1089 obtained in rat liver postmitochondrial supernatant fraction (——, EB1446). The peak at 9.26 min represents 1,25-$(OH)_2D_3$, which was used as an internal standard. The peaks were resolved on a Zorbax-CN column (25 × 0.46 cm, 6 μ); solvent system used was HIM, 88:10:2, at a flow rate of 1 mL/min.

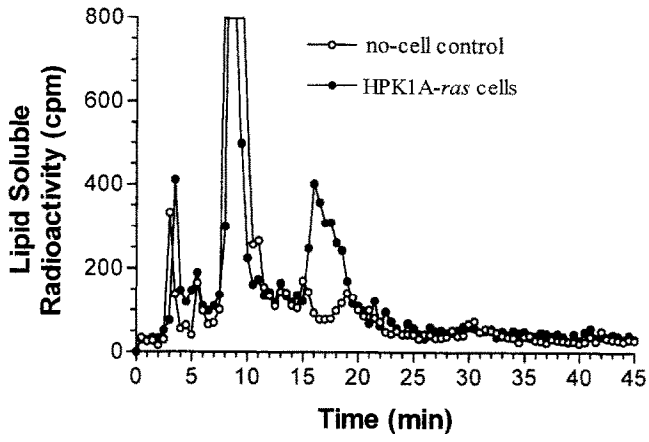

FIG. 7. HPLC profile of the lipid extract from HPK1A-*ras* cells incubated with [19-^{14}C]EB1089. Total lipid extract from a 72-hr incubation was separated on a Zorbax-SIL column using the solvent HIM 91:7:2 at a flow rate of 1 mL/min. [19-^{14}C]Metabolites of EB1089 were identified based upon their comigration with synthetic standards. HPK1A-*ras* cells with [19-^{14}C]EB1089, ●; no-cell control, ○.

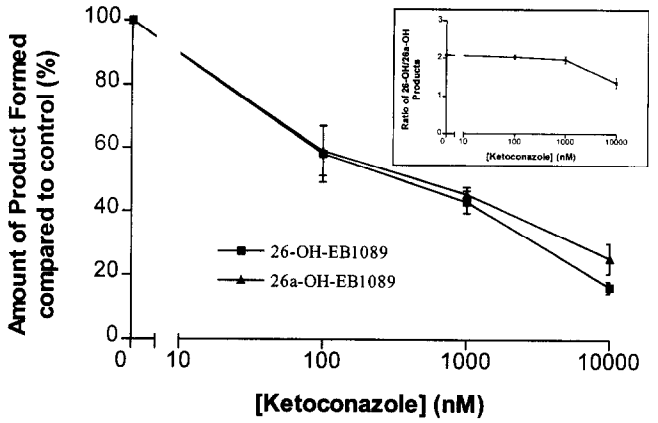

FIG. 8. Cytochrome P450 inhibition studies. Incubations of HPK1A-*ras* cells with EB1089 were carried out in the absence (control) and presence of ketoconazole at the specified concentrations. Amounts of metabolites formed were monitored by HPLC on a Zorbax-SIL column using the solvent HIM 91:7:2 at a flow rate of 1 mL/min. The inset denotes the ratio of the principal metabolites 26-OH-EB1089: 26a-OH-EB1089 formed at the specified concentrations of ketoconazole.

series of fragments at m/z 587/497/407/317, due to cleavage between C-24 and C-24a $(M-173)^+$ followed by successive loss of silanols. This series is found in other 24-hydroxylated vitamin D analogs, such as the homologated vitamin D compounds [22]. This series of fragments strongly suggests that the extra hydroxyl must be at C-24 and, hence, the metabolite (peak A) is probably 24-hydroxy MC1473.

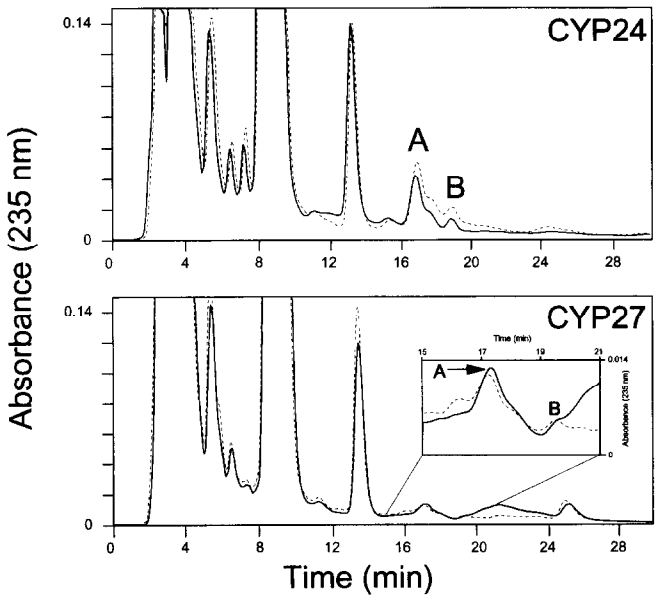

FIG. 9. COS-1 transfection cell experiments, using vectors containing CYP27 and CYP24, incubated with EB1089. Peak A and Peak B denote the formation of 26-hydroxy EB1089 and 26a-hydroxy EB1089, respectively, in the presence of transfected cytochromes (----) and in control experiments (——). In the lower panel, the inset represents a magnification of the product portion of the traces.

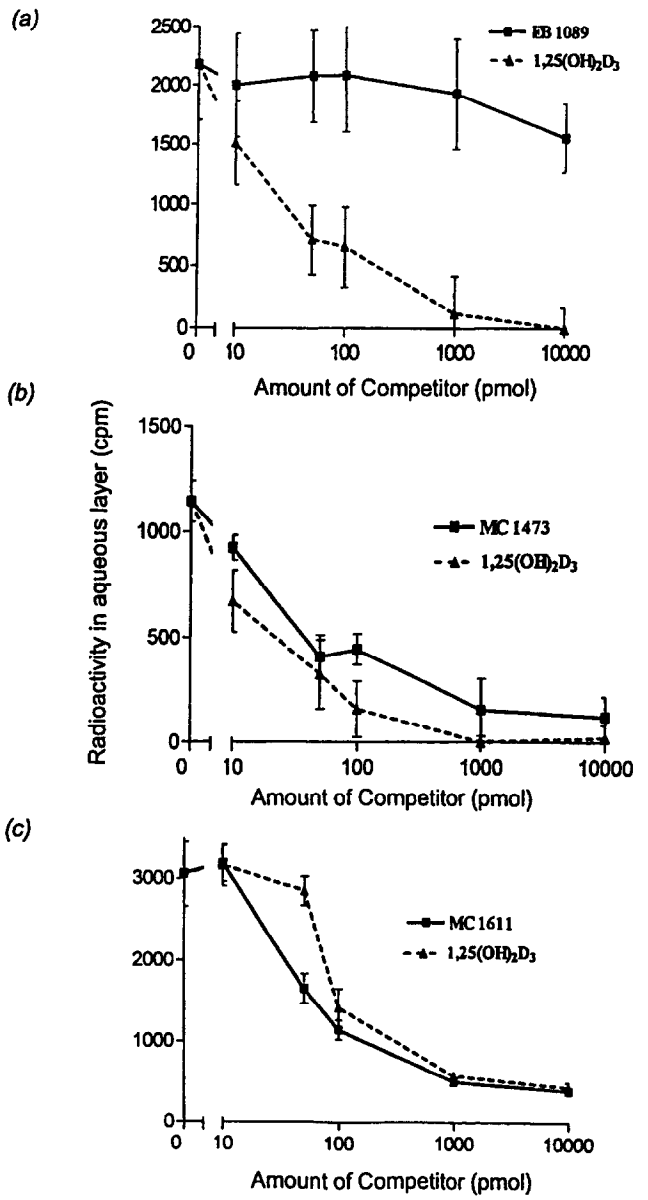

FIG. 10. Competitive metabolism experiments using nonradioactive (a) EB1089, (b) MC1473, and (c) MC1611 in HPK1A-*ras* cells. [1β-^{3}H]1,25-$(OH)_2D_3$ was incubated in HPK1A-*ras* cells in the presence of vehicle alone or varying concentrations of EB1089, MC1473, MC1611, or 1,25-$(OH)_2D_3$. Incubations were performed as described in Materials and Methods. Each point in the figure is the mean ± SE of 3 flasks counted in triplicate.

The metabolic pattern for HPK1A-*ras* with MC1611 (Fig. 11c) showed the formation of 1 major metabolite (peak A) and 1 minor metabolite (peak B). The mass spectrum of the pertrimethylsilylated derivative of peak A (Fig. 11d) showed a molecular ion of m/z 760, indicating a hydroxylated version of MC1611. Important fragments include m/z at 287 and 197 $(287-90)^+$, which arise from the cleavage between C-22 and C-23 and series of fragments at m/z 731/641/551/461/371, which arise from the cleavage between C-26 and C-26a followed by the successive loss of up to 4 silanol groups. Also observed in the mass spectra are

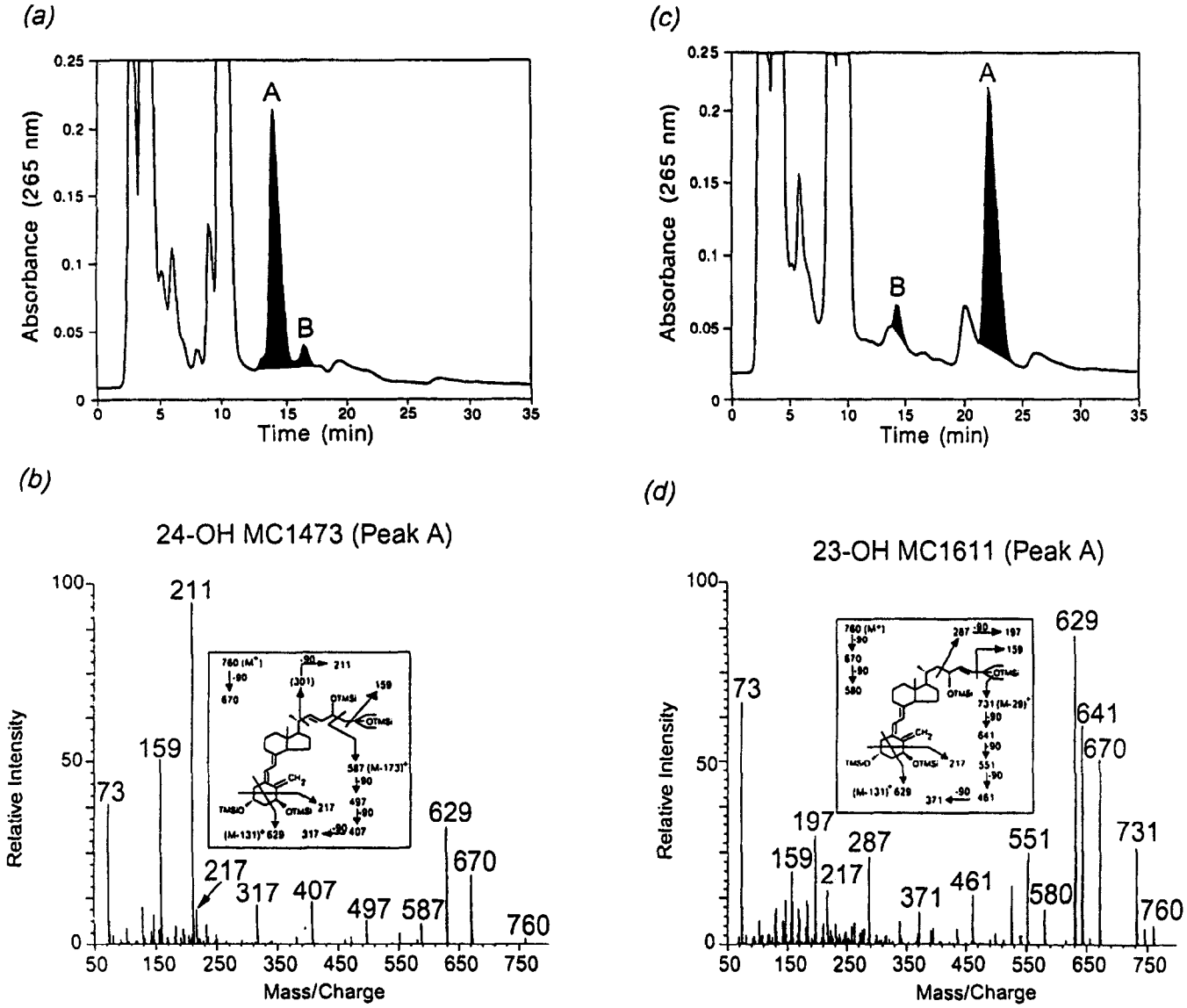

Fig. 11. (a) and (c) HPLC profiles of lipid extracts from HPK1A-*ras* cells incubated with MC1473 and MC1611, respectively. Total lipid extracts were separated on a Zorbax-SIL column using the solvent HIM 91:7:2 at a flow rate of 1 mL/min. Metabolites of MC1473 and MC1611 were identified based on their characteristic vitamin D chromophore (λ_{max} = 265 nm, λ_{min} = 228 nm, $\lambda_{max}/\lambda_{min}$ = 1.75), and have been shaded. (b) and (d) Mass spectra of the putative metabolites, 24-OH MC1473 and 23-OH MC1611. See Fig. 3 legend for details.

fragments at m/z 629 $(M-131)^+$, 670 $(M-90)^+$, 580 $(M-90-90)^+$, and 159 (cleavage between C-24a and C-25). Absent from this spectrum are the m/z 103 and 117 fragments observed in the spectra of 26-OH-EB1089 and 26a-OH-EB1089. Based on these observations, peak A has been identified as 23-hydroxy MC1611.

Thus, it appears that MC1473 is subjected to 24-hydroxylation while MC1611 is mainly 23-hydroxylated.

DISCUSSION

In this paper, we have demonstrated that EB1089 is metabolized by 2 different cultured human cells to side-chain hydroxylated metabolites identified as 26-hydroxy EB1089 and 26a-hydroxy EB1089. Their identification rested on two different approaches, one involving direct interpretation of mass spectral evidence acquired from GC-MS and the other from cochromatography of the metabolites with chemically synthesized authentic standards. In the companion paper to this, Kissmeyer *et al.* [24] used different biological systems *in vivo* and *in vitro*, and different identification strategies using NMR, as well as cochromatography, with the same chemically synthesized standards to reach identical conclusions. Though the hydroxylation of vitamin D metabolites in the 26-position has been reported in earlier metabolic studies, this type of modification has been associated with the liver and rarely found in vitamin D-target cells, except in the context of 26,23-lactone formation [25, 26]. To the best of our knowledge, this is the first time 26a-hydroxylation of a vitamin D metabolite has been

reported. The metabolic pathway operates at nanomolar and micromolar concentrations of analog. One interesting feature of mammalian cell (HPK1A-*ras*) metabolism is that the observed hydroxylations (at C-26 and 26a) are stereo-specific. Out of four possible diastereomers of 26-hydroxy EB1089 and two epimers of 26a-hydroxy EB1089, only one diastereomer of 26-hydroxy EB1089 (EB1445; 25R,26R) and one epimer of 26a-hydroxy EB1089 (EB 1435a; 25-configuration unknown) are formed. The metabolism observed in the hepatoma cell model here and in the rat liver postmitochondrial preparations in the companion paper [24] is less stereo-specific though, again, a single diastereomer with 26R-hydroxy stereochemistry predominates.

This leads one to consider if these hydroxylations are carried out by cytochromes and, if so, whether or not CYP27 and/or CYP24 are involved. Studies with ketoconazole (at varying concentrations) resulted in the inhibition of these hydroxylations, thereby suggesting that cytochromes P450s *are* involved. However, transfection experiments in COS-1 cells failed to generate significant quantities of 26- and 26a-OH EB1089, suggesting that the specific isoforms CYP27 and CYP24 are probably not involved in these hydroxylations. The results of catabolic assay experiments in the presence of [1β-^{3}H]1,25-$(OH)_2D_3$ showed a lack of competition by EB1089, implying a lack of involvement of CYP24 in these hydroxylations, a suggestion that has also been made by others [27]. Therefore, it is likely that these hydroxylations of EB1089 are carried out by some unrelated cytochrome P450s.

The studies on the metabolism of partially reduced versions of EB1089, in the work on MC1473 and MC1611, have led to a plausible hypothesis to explain the redirecting of hydroxylation from the 23- and 24-positions, normally targeted in the vitamin D side chain, to the 26- and 26a-carbons. Using the nonconjugated analogs, MC1473 and MC1611, we obtained 24-hydroxy MC1473 and 23-hydroxy MC1611, respectively, as the principal products. Because these analogs, like EB1089, both contain 26,27-dimethyl groups and 24a-homologation in the side-chain, differing only in their lack of the conjugated diene, it is tempting to conclude that changes in hydroxylation regioselectivity must be due to the conjugated diene of EB1089. Though it is possible that small amounts of metabolites that have lost the UV-chromophore of EB1089 could be present in our extracts, no major peaks were found with the classical vitamin D chromophore (λ_{max} = 265 nm, λ_{min} = 228 nm). Moreover, incubations with [^{14}C]EB1089 indicate that 26 and 26a-hydroxylations are the predominant reactions occurring in mammalian cells. Thus, it appears that the conjugated diene is responsible for blocking hydroxylation at C-23 and C-24. It is also possible that since 23- and 24-hydroxylations are blocked in EB1089, other structural features, such as the terminal ethyl groups, encourage the enzymes responsible to hydroxylate at C-26 and C-26a. In this respect, it is interesting to note that another homologated vitamin D analog, MC1548, with a classical vitamin D side-chain containing only the 26,27-dimethyl group, but no double bonds at all, has been found to be 26-hydroxylated as well as being subject to 23- and 24-hydroxylation [28]. In this case, no evidence was found for 26a-hydroxylation. Studies such as these, which pinpoint the structural features responsible for changes in metabolism, will help to establish a more rational approach to vitamin D drug design from a metabolic perspective.

Along with the companion paper, this work has important implications for the use of EB1089 as a drug *in vivo*. For the first time, we have conclusively identified a metabolite of EB1089 in a biological system. Earlier studies [29] using radioactive EB1089 established the complexity of the metabolic profile and chromatographic behaviour of the metabolites and the fact that metabolites could be formed *in vitro* and *in vivo*. However, the metabolic work reported here and in the companion paper [24] provided the impetus to chemically synthesize 26- and 26a-hydroxylated EB1089 standards and, thus, be in a position to establish the biological activity and other properties of the metabolites identified here. In fact, the chemical synthesis of all of the possible diastereomers of 26-OH-EB1089 and epimers of 26a-OH-EB1089 also allowed for the determination of their biological activity in cell-proliferation and calcemic assays reported in the companion paper [24]. The biological activity studies of EB1089 metabolites reported here set the stage for other, more sophisticated, transactivation assays previously carried out for the parent compound, EB1089 [30]. These studies may allow us to evaluate whether the full biological effects of EB1089 are due to the parent compound or its metabolites.

The current studies using cultured human cells re-emphasize another property of EB1089 previously observed in animal studies, namely its relatively long half-life *in vivo* compared to other vitamin D analogs. In our intact cell systems, EB1089 was extremely stable. It appears that the resistance of the conjugated diene system to the action of 23- and 24-hydroxylases must be at least partially responsible for this phenomenon because 1,25-$(OH)_2D_3$ and a variety of other vitamin D compounds, including the 2 partially reduced analogs, MC1473 and MC1611, and the 26,27-dimethyl analog MC1548 [28], are all subject to more rapid metabolism than is EB1089 by these hydroxylases. It will be interesting to see if part of the promising drug profile of EB1089 *in vivo*, including its long half-life compared to other vitamin D analogs, is due to its relative stability to liver and target-cell catabolic enzymes. Various clinical trials of EB1089 are currently underway. Provision of the details of the metabolic fate of EB1089 can only lead to safer and more effective use of this interesting compound as a drug in such trials.

This work was supported by grants from the Medical Research Council of Canada and Leo Research Foundation, Ballerup, Denmark. We acknowledge the important contribution of Drs. Richard Kremer, Department of Medicine, McGill University, Montreal, Québec, Canada and Johng Rhim, NCI, National Institutes of Health, Bethesda, MD,

U.S.A. in the development of the HPK1A-ras cell line used in this work.

References

1. Shankar VN, Makin HLJ, Schroeder NJ, Trafford DJH, Kissmeyer A-M, Binderup E, Calverley MJ and Jones G, Metabolism of the antiproliferative vitamin D analogue, EB1089, in a cultured human keratinocyte model. *Bone* **17:** 326 (Abst. P27), 1995.
2. Shankar VN, Makin HLJ, Schroeder NJ, Trafford DJH, Kissmeyer A-M, Binderup E, Calverley MJ and Jones G, Metabolism of vitamin D analogs containing side chain double bonds: conjugated system of EB1089 blocks 24-hydroxylation. *J Bone Mineral Res* **10:** S389 (Abst. M548), 1995.
3. Suda T, Shinki T and Takahashi N, The role of vitamin D in bone and intestinal cell differentiation. *Annu Rev Nutr* **10:** 195–211, 1990.
4. Calverley MJ, Synthesis of MC903, a biologically active vitamin D metabolite analogue. *Tetrahedron* **43:** 4609–4619, 1987.
5. Abe J, Morikawa M, Miyamoto K, Kaiho S, Fukushima M, Miyaura C, Abe E, Suda T and Nishii Y, Synthetic analogs of vitamin D_3 with an oxygen atom in the side chain skeleton: a trial of the development of vitamin D compounds which exhibit potent differentiation activation activity without inducing hypercalcemia. *FEBS Lett* **226:** 58–62, 1987.
6. Bretting C, Calverley MJ and Binderup L, Synthesis and biological activity of 1α-hydroxylated vitamin D_3 analogues with hydroxylated side chains, multi-homologated in the 24- or 24,26,27-positions. In: *Vitamin D_3 Gene Regulation, Structure Function Analysis and Clinical Applications, Proceedings of the Eighth Workshop on Vitamin D, Paris, France, 5–10 July 1991.* (Eds. Norman AW, Bouillon R and Thomasset M), pp. 159–162, Walter de Gruyter, Berlin, 1991.
7. Dilworth FJ, Calverley MJ, Makin HLJ and Jones G, Increased biological activity of 20-epi-1,25-dihydroxyvitamin D_3 is due to reduced catabolism and altered protein binding. *Biochem Pharmacol* **47:** 987–993, 1994.
8. Lohnes D and Jones G, Side chain metabolism of vitamin D_3 in osteosarcoma cell line UMR-106. *J Biol Chem* **262:** 14394–14401, 1987.
9. Akiyoshi-Shibata M, Sakaki T, Ohyama Y, Noshiro M, Okuda K and Yabusaki Y, Further oxidation of hydroxycalcidiol by calcidiol 24-hydroxylase—A study with the mature enzyme expressed in *Escherichia coli*. *Eur J Biochem* **224:** 335–343, 1994.
10. Binderup E, Calverley MJ and Binderup L, Synthesis and biological activity of 1α-hydroxylated vitamin D analogues with poly-unsaturated side chains. In: *Vitamin D_3 Gene Regulation, Structure Function Analysis and Clinical Applications, Proceedings of the Eighth Workshop on Vitamin D, Paris, France, 5–10 July 1991.* (Eds. Norman AW, Bouillion R and Thomasset M), pp. 192–193, Walter de Gruyter, Berlin, 1991.
11. Mathiasen IS, Colston KW and Binderup L, EB1089, a novel vitamin D analogue has strong antiproliferative and differentiation-inducing effects on cancer cells. *J Steroid Biochem Molec Biol* **46:** 365–371, 1993.
12. James SY, Mackay AG, Binderup L and Colston KW, Effects of a new synthetic analogue, EB1089, on the oestrogen-responsive growth of human breast cancer cells. *J Endocr* **141:** 555–563, 1994.
13. Masuda S, Strugnell S, Calverley M, Makin HLJ, Kremer R and Jones G, *In vitro* metabolism of the anti-psoriatic vitamin D analog, calcipotriol, in two cultured human keratinocyte models. *J Biol Chem* **269:** 4794–4803, 1994.
14. Makin G, Lohnes D, Byford V, Ray R and Jones G, Target cell metabolism of 1α,25-dihydroxyvitamin D_3 to calcitroic acid. *Biochem J* **262:** 173–180, 1989.
15. Henderson J, Sebag M, Rhim J, Goltzman D and Kremer R, Dysregulation of parathyroid hormone-like peptide expression and secretion in a keratinocyte model of tumour progression. *Cancer Res* **51:** 6521–6528, 1991.
16. Sebag M, Henderson J, Rhim J and Kremer R, Relative resistance to 1,25-dihydroxyvitamin D_3 in a keratinocyte model or tumour progression. *J Biol Chem* **267:** 12162–12167, 1992.
17. Bligh EG and Dyer WJ, A rapid method of total lipid extraction and purification. *Can J Biochem* **37:** 911–917, 1957.
18. Qaw F, Calverley MJ, Schroeder NJ, Trafford DJH, Makin HLJ and Jones G, *In vivo* metabolism of the vitamin D analog, dihydrotachysterol. *J Biol Chem* **268:** 282–292, 1993.
19. Sambrook J, Fritsch EF and Maniatis T, In: *Molecular Cloning: a Laboratory Manual.* 2nd Ed, pp. 16.42–16.44. Cold Spring Harbor Laboratories, Cold Spring Harbor, NY, 1989.
20. Guo Y, Strugnell S, Back D and Jones G, Transfected human liver cytochrome P450 hydroxylates vitamin D analogs at different side-chain positions. *Proc Natl Acad Sci USA* **90:** 8668–8672, 1993.
21. Ohyama Y, Noshiro M and Okuda K, Cloning and expression of cDNA encoding 25-hydroxyvitamin D_3 24-hydroxylase. *FEBS Lett* **278:** 195–198, 1991.
22. Dilworth FJ, Scott I, Green A, Strugnell S, Guo Y-D, Roberts EA, Kremer R, Calverley MJ, Makin HLJ and Jones G, Different mechanisms of hydroxylation site selection by liver and kidney cytochrome P-450 species (CYP27 and CYP24) involved in vitamin D metabolism. *J Biol Chem* **270:** 16766–16774, 1995.
23. Makin HLJ, Jones G and Calverley MJ, Analysis of Vitamin D, its metabolites and structural analogues. In: *Steroid Analysis* (Eds. Makin HLJ, Gower DB and Kirk DN), pp. 562–620. Blackie, Glasgow, 1995.
24. Kissmeyer A-M, Binderup E, Binderup L, Hansen CM, Rastrup-Andersen N, Makin HLJ, Shankar VN and Jones G, The metabolism of the vitamin D analog EB1089: Identification of *in vivo* and *in vitro* liver metabolites and their biological activities. *Biochem Pharmacol* **53:** 000–000; 1997.
25. Yamada S, Nakayama K, Takayama H, Shinki T, Takasaki Y and Suda T, Isolation, identification and metabolism of (23S,25R)-25-hydroxyvitamin D_3-26,23-lactol: a biosynthetic precursor of (23S,25R)-25-hydroxyvitamin D_3-26,23-lactone. *J Biol Chem* **259:** 884–889, 1984.
26. Ishizuka S, Oshida J-I, Tsuruta H and Norman AW, The stereochemical configuration of the natural 1-alpha,25-dihyroxyvitamin D_3-26,23-lactone. *Arch Biochem Biophys* **242:** 82–89, 1985.
27. Roy S, Martel J and Tenenhouse HS, Comparative effects of 1,25-dihydroxyvitamin D_3 and EB1089 on mouse renal and intestinal 25-hydroxyvitamin D_3-24-hydroxylase. *J Bone Mineral Res* **10:** 1951–1958, 1995.
28. Dilworth FJ, Scott I, Calverley MJ, Makin HLJ and Jones G, Enzymes of side chain oxidation pathway not affected by addition of methyl groups to end of the vitamin D_3 side chain. *J Bone Mineral Res* **10:** S388 (Abst. M546), 1995.
29. Kissmeyer A-M, Shankar VN, Jones G and Makin HLJ, The *in vitro* and *in vivo* metabolism of EB1089. *Bone* **17:** S327 (Abst. P29), 1995.
30. Carlberg C, Mathiasen IS, Saurat JH and Binderup L, The 1,25-dihydroxyvitamin D_3 (VD) analogues MC903, EB1089, and KH1060 activate the VD receptor: homodimers show higher ligand sensitivity than heterodimers with retinoid X receptors. *J Steroid Biochem Molec Biol* **51:** 137–142, 1994.